ACADEMIC
PRESS

Available online at www.sciencedirect.com
SCIENCE DIRECT®

Journal of Catalysis 214 (2003) 234–241

JOURNAL OF
CATALYSIS

www.elsevier.com/locate/jcat

Initial steps in the desulfurization of thiophene/Ni(100)—A DFT study

F. Mittendorfer [a,b,*] and J. Hafner [a]

[a] *Institut für Materialphysik and Center for Computational Materials Science Universität Wien, Sensengasse 8/12, A-1090 Vienna, Austria*
[b] *Institut Français du Pétrole, 1&4 Avenue de Bois-Préau, 92852 Rueil-Malmaison, France*

Received 31 July 2002; revised 30 October 2002; accepted 30 October 2002

Abstract

The desulfurization of thiophene on a Ni(100) surface has been studied using ab initio local-density-functional calculations. The calculations were performed using the Vienna ab initio simulation package (VASP), which is based on a plane wave basis set and PAW potentials. Starting from preadsorbed thiophene on the nickel surface several reaction pathways for the desulfurization of the thiophene molecule mechanism have been investigated: In the optimized reaction path an energetic barrier of 0.71 eV has been found for this reaction step. In addition the influence of a hydrogenation of the molecule after the initial C–S bond cleavage was investigated. Although the hydrogenation is predicted to lower the barrier for the desulfurization to 0.14 eV, the barrier for the hydrogenation itself, 0.98 eV, disfavors this process. A detailed analysis of the structural and electronic properties of the molecule in the corresponding transition states is presented.

Keywords: Density functional calculations; Chemisorption; Aromatics; Single crystal surfaces; Metallic surfaces

1. Introduction

Although the processing of petrochemical products has a long tradition, environmental regulations have led to an increased effort to reduce sulfur levels in fuels. Petroleum feedstocks contain a wide range of sulfur containing aromatic molecules like thiophene. A well-known industrial technology used for desulfurization is the hydrodesulfurization process (HDS), in which sulfur-containing molecules react with hydrogen in the presence of a catalyst:

$$C_mH_nS + xH_2 \rightarrow H_2S + \text{hydrocarbons}.$$

Thiophene is often used as a test molecule for this process. The mechanisms for the hydrodesulfurization (HDS) reaction of thiophene have been discussed in a number of reviews [1–3]:

- The first reaction mechanism starts with hydrogenation of the thiophene ring to form a 2,3-dihydrothiophene intermediate [4].
- Alternatively a direct hydrogenolysis of the C–S bond is assumed, resulting in the formation of 1,3-butadiene (C_4H_6) [5].
- An additional proposal [6] is derived from the organometallic reaction of Cp*Ir(2,5-dimethylthiophene) with iron carbonyls ($Cp^* = \eta^5 - C_5Me_5$). In this model the initial step of the HDS is the C–S bond cleavage associated with an incorporation of the metal atom into a six-membered ring.

Generally supported sulfides such as molybdenum disulfide (MoS_2) are used to catalyze this reaction, often promoted with Co or Ni [2]. Although pure transition metal surfaces such as Ni show catalytic activity for hydrogenation processes, the difficulty of removing the adsorbed sulfur makes them unsuitable for industrial hydrodesulfurization. Yet a number of recent studies has been dedicated to the investigation of the desulfurization of thiophene over well-defined Ni surfaces to gain detailed insights into fundamental aspects of the desulfurization.

Huntley et al. [7] report in a recent study of thiophene/Ni(111) based on X-ray photoelectron spectroscopy (XPS) and high-resolution electron energy loss spectroscopy (HREELS) a cleavage of the C–S bond at 150 K. They observe a hydrocarbon intermediate; still they are unable to differentiate between a “true” metallocycle involving one metal atom and a hydrocarbon bound in a bidentate fashion to two metal centers. Zaera and co-workers [8] have studied the adsorption of thiophene on Ni(100) with near-edge X-ray ad-

---

[*] Corresponding author.
E-mail address: florian.mittendorfer@ifp.fr (F. Mittendorfer).

0021-9517/03/$ – see front matter
doi:10.1016/S0021-9517(02)00149-5

sorption (NEXAFS) and HREELS experiments and report a scission of the S–C bond at temperatures below 90 K. Khan et al. [9] have investigated the HDS activity of Ni/Pt(111) surfaces in a recent TPD study. While Neurock and van Santen discussed several aspects of the hydrodesulfurization of thiophene at Ni_xS_y with the help of cluster calculations [10], important issues such as the reaction paths and the energy barriers for the process over a metal surface are still open.

Hence the catalytic properties of the surface will be investigated in the following sections: after a description of the methodology, the steps of the investigated reaction will be discussed. In the next section the decomposition of the molecule will be covered and in the final section the influence of coupled hydrogenation–desulfurization on the reaction barriers will be analyzed.

2. Methodology

The calculations were performed using the Vienna ab initio simulation package (VASP) [11,12]. VASP performs an iterative solution of the Kohn–Sham equations of the density functional theory (DFT) using residuum-minimization techniques and optimized charge-density mixing routines. The program uses a plane-wave basis set, thus offering good access to the Hellmann–Feynman forces acting on the atoms. The calculations were performed using the projector-augmented wave (PAW) method [13,14] and generalized gradient (GGA) corrections as proposed by Perdew et al. [15]. For the plane wave set a cutoff energy of 400 eV was used.

The Brillouin-zone integrations have been performed using a $4 \times 4 \times 1$ Monkhorst–Pack grid [16] and Methfessel–Paxton smearing [17] of 0.1 eV. The convergence of this setup has been confirmed by previous studies of the adsorption of aromatic molecules on transition metal surfaces [18,19]. The calculations were performed for a nonmagnetic nickel substrate as the magnetization did not show a significant influence on the calculated reaction barriers for hydrogenation reactions [20]. For the nonmagnetic Ni substrate the calculated DFT-GGA lattice constant of $r_0 = 3.52$ Å has been used.

The supercell was chosen corresponding to a $c(4 \times 4)$ superstructure of the adsorbed thiophene molecules, the surface was modeled by a five-layer slab with the uppermost layer allowed to relax. For the reference system sulfur was calculated in a $p(2 \times 2)$ superstructure on a five-layer slab.

The transition states of the reaction were determined using the nudge-elastic-band method [21], which is based on an explicit mapping of the reaction path. For each reaction step a set of eight images was used. In addition the image closest to the transition state has been relaxed using a quasi-Newton algorithm to obtain the transition state. The transition states were verified by the calculation of the vibrational frequencies within an harmonic approach.

3. Reaction steps for the desulfurization of thiophene/Ni(100)

The interaction of the molecule with the metallic surface plays a crucial role in the desulfurization of the molecule: in the case of thiophene/Ni(100) the molecule adsorbs with its π-ring parallel to the surface, and the strong weakening of the intramolecular bonds is predicted to result in the barrierless rupture of one of the S–C bonds upon the adsorption of the molecule [18]. The S atom and the terminal atom of the now linear molecule are bound to the substrate in near-bridge positions, with a mutual distance of 2.90 Å (see panel A in Fig. 1). The bond length of the remaining S–C bond is elongated from a calculated gas-phase value of 1.72 Å to a value of 1.80 Å. Stöhr et al. have shown in their X-ray studies that the thiophene molecules will dissociate upon adsorption onto an Ni(100) surface already at temperatures as low as 100 K [22]. Zaera et al. [8] have observed a S–C bond breaking at 90 K, followed by a dehydrogenation of the hydrocarbon fragment to C_4H_3 in a temperature range from 230 to 500 K, and finally a complete decomposition at 650 K. Yet this paper will be dedicated to

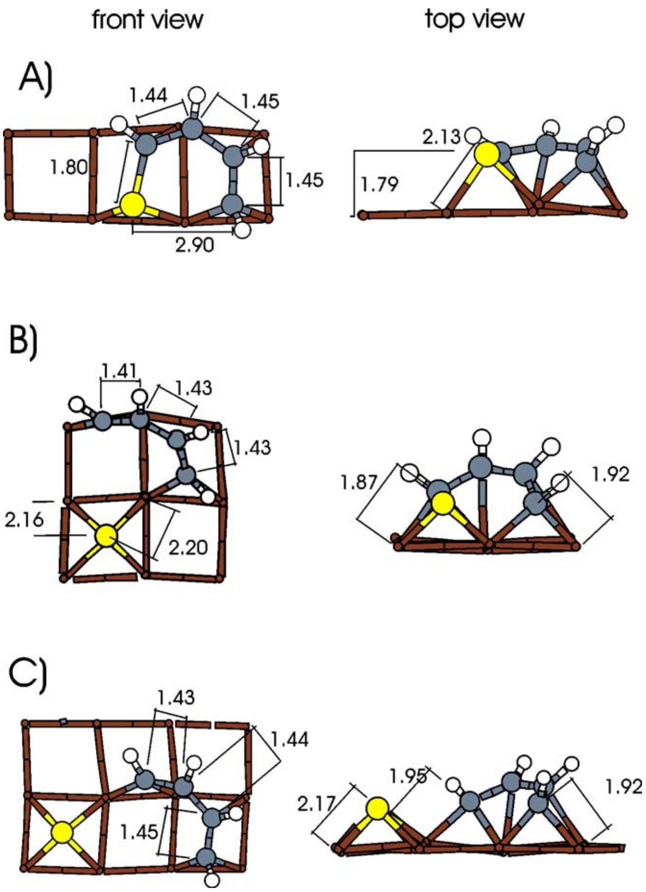

Fig. 1. Thiophene adsorbed on a Ni(100) surface: Adsorption geometry (A) at the initial bridge position with one broken S–C bond, (B) after the second S–C bond scission and the diffusion of the sulfur atom into the neighboring hollow site, and (C) after the second S–C scission and sulfur diffusion into an alternative hollow site.

Table 1
Adsorption energy and structural parameters of selected adsorbates on a Ni(100) surface: atomic sulfur adsorbed in the hollow position (S), thiophene adsorbed in the bridge position with one broken C–S bond (thiophene) and final products after a second C–S bond scission, i.e., an S atom and a C_4H_4 fragment in the two configurations shown in Fig. 1

	E_{ads} (eV)	d(S–Ni) (Å)	d(C–Ni) (Å)
S[a]	2.68	2.18	–
Thiophene, (A,B–S)	2.57	2.13	1.87–2.03
S + C_4H_4, conf. 1 (A–E)	3.10	2.16/2.20	1.88–2.29
S + C_4H_4, conf. 2 (B–E)	3.18	2.17/2.19	1.88–2.26

[a] The adsorption energy for sulfur/Ni(100) is given with respect to H_2S; i.e., $E_{ads} = E(\mathrm{S/Ni(100)}) + E_B(H_2)_{gas} - E(\mathrm{Ni(100)}) - E_B(H_2S)_{gas}$.

the description of the desulfurization itself, therefore only reaction pathways starting from the adsorbed molecule and ending with coadsorbed S and C_4H_4 will be investigated. The computational setup for this study has been described in the previous section.

As the adsorption of atomic sulfur on Ni(100) is energetically preferred in the hollow site, the geometry of the adsorbed thiophene molecule (Fig. 1) favors an obvious reaction path: As the adsorption process results already in the scission of one of the S–C bonds and the sulfur atom is located at the bridge position, an elongation of the remaining S–C bond moves the sulfur atom into the favored hollow site. An alternative reaction path is based on the other neighboring hollow site as final position for the sulfur atom.

Table 1 gives a comparison of the energetic data and the adsorption geometries of the final hydrocarbon fragments to those of the initially adsorbed thiophene molecule. The desulfurization is favored from an energetic viewpoint: the reaction along the short pathway increases the adsorption energy by 0.53 eV; the reaction along the longer pathway into the other hollow position results in an energy gain of 0.61 eV.

In both cases the sulfur is finally adsorbed in the the hollow position with a S–Ni distance of $d(\text{S–Ni}) = 2.17$ Å, nearly the same value as for the low-coverage $p(2 \times 2)$ adsorption of atomic sulfur ($d(\text{S–Ni}) = 2.18$ Å). For both fragments the S–Ni and C–Ni bonds are not completely symmetric as one nickel atom interacts with both the S-atom and the hydrocarbon fragment.

For both desulfurized cases the remaining C_4H_4 hydrocarbon fragment is no longer parallel to the surfaces (Fig. 1). The carbon atoms at both ends of the chain, located in bridge positions, form strong bonds to the substrate with Ni–C bond lengths ranging from 1.87 to 1.94 Å, whereas of the two central carbon atoms of the hydrocarbon fragment one is located close to an on-top position and the other halfway between a bridge and a hollow-site; both form only weaker surface bonds with bond lengths ranging from 2.15 to 2.30 Å.

In contrast to the uniform expansion of the carbon–carbon bonds to 1.45 Å in the adsorbed thiophene, the carbon–carbon distances in the C_4H_4 fragments are again slightly decreased to about 1.43 Å, reflecting an increase in the bondstrength of the C–C bonds.

4. Reaction pathway for the desulfurization of thiophene/Ni(100)

Although the results of the last section have shown that the desulfurization of thiophene/Ni(100) is favored from the point of energetics, little is known about the desulfurization process itself. Especially, the energetic barrier of the reaction has a crucial role for the reaction kinetics. Consequently the determination of the transition state of the reaction is of central importance for the comparison of various reaction paths. As mentioned in Section 2, all reaction pathways have been determined using the nudged-elastic-band method.

The first reaction path that has been investigated within this work is displayed in Fig. 2. This mechanism allows the shortest reaction path: Since the sulfur atom is already located over a bridge site upon adsorption (A–S), an elongation of the S–C bond steers the sulfur atom into the adjacent hollow position. Fig. 2 gives the energetic profile of the reaction: the barrier for this mechanism is found to be $E_{barr} = 0.84$ eV; the energy gain with respect to the initial adsorption position is 0.53 eV.

Details of the geometric structure of the transition state (A–TS) are given in Fig. 3. The structure of the transition state is determined by two competing trends along the reaction pathway: On the one hand the energy gain by the motion of the sulfur atom from the bridge position into the hollow position, which is larger than $\Delta E_{ads} = 1$ eV for S/Ni(100); on the other hand an energy loss caused by the elongation of the S–C bond. In addition the intramolecular bonds have already been weakened by the original formation of bonds between the thiophene molecule and the substrate. Although the sulfur–carbon bond is stretched to 2.50 Å at the transition state the sulfur atom is still close to the bridge position, as the α carbon in turn is also involved in bonds to the substrate with bond lengths of $d(\text{C–Ni}) = 1.96$, respectively 1.98 Å.

An analysis of the electronic properties at the transition state completes this picture. Fig. 4 gives a comparison of the local density of states (DOS) of the initially adsorbed molecule and the DOS at the transition state projected on the carbon atoms starting from C1 at the end of the hydrocarbon chain to C4 close to the sulfur atom resp. on the sulfur atom itself.

The bond between the sulfur atom and the hydrocarbon fragment is nearly broken at the transition state: the hybridization between the carbon and sulfur s-states that lead to the formation the molecular orbitals is lifted and only a rehybridization between the carbon molecules is found. The density of states of the sulfur atom shows already the bonding expected for atomically adsorbed sulfur: the sulfur s-electrons form a single state with a binding energy of -13 eV, while the p-orbitals hybridize mainly with the nickel d-states.

In addition to the previously discussed reaction pathway a supplementary scenario has been investigated: starting again from an adsorption of the thiophene molecule in the bridge position (B–S) the sulfur atom is translated

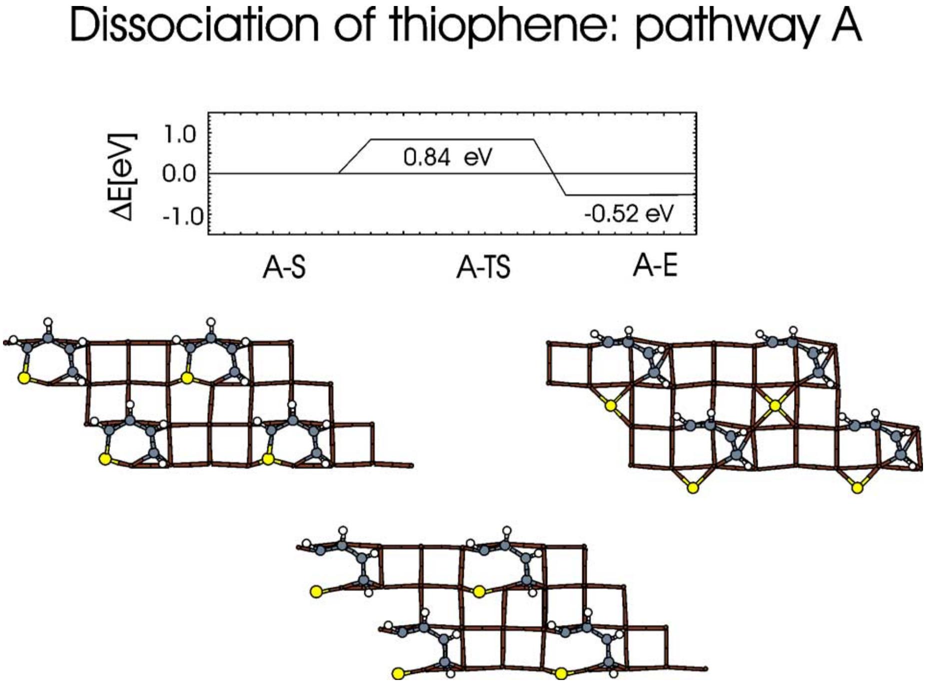

Fig. 2. Desulfurization of thiophene/Ni(100): Energetic profile along the reaction path A starting from the reactants in the initial adsorption position (A–S), followed by the transition state (A–TS) and the desulfurized molecule in the final position (A–E).

via the second bridge site to the alternative neighboring hollow site (Fig. 5). In contrast to the previously discussed path this reaction takes place in two steps: An initial step in which the hydrocarbon fragment is deformed nearly barrierlessly into a metastable intermediate (B–I1) with the sulfur atom located at the free bridge site (Fig. 6). Although the transition state for this step has not been identified explicitly, the forces along the reaction path indicate that that the transition state, located close to the intermediate (B–I1), has an energetic barrier of less than 50 meV for the back-reaction from the intermediate to the initial configuration. The structure of this intermediate (B–I1) as shown in Fig. 6A is similar to the original adsorption position: the sulfur atom is located at the neighboring bridge site, the length of the S–C bond is $d(\text{S–C}) = 1.80$ Å and the distance between the sulfur and nearest Ni atoms is $d(\text{S–Ni}) = 2.14$ Å, respectively $d(\text{S–Ni}) = 2.22$ Å. Like in the initial starting configuration the carbon chain is nearly parallel to the surface; the intramolecular carbon–carbon distances range from $d(\text{C–C}) = 1.44$ to 1.46 Å.

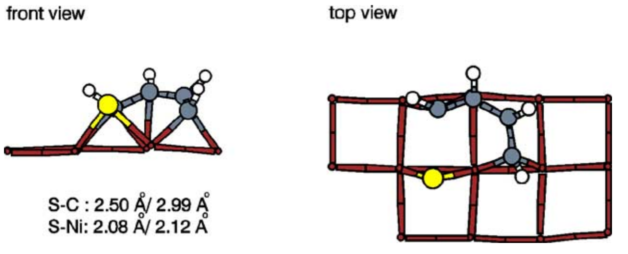

Fig. 3. Desulfurization of thiophene/Ni(100): structure of the transition state (A–TS).

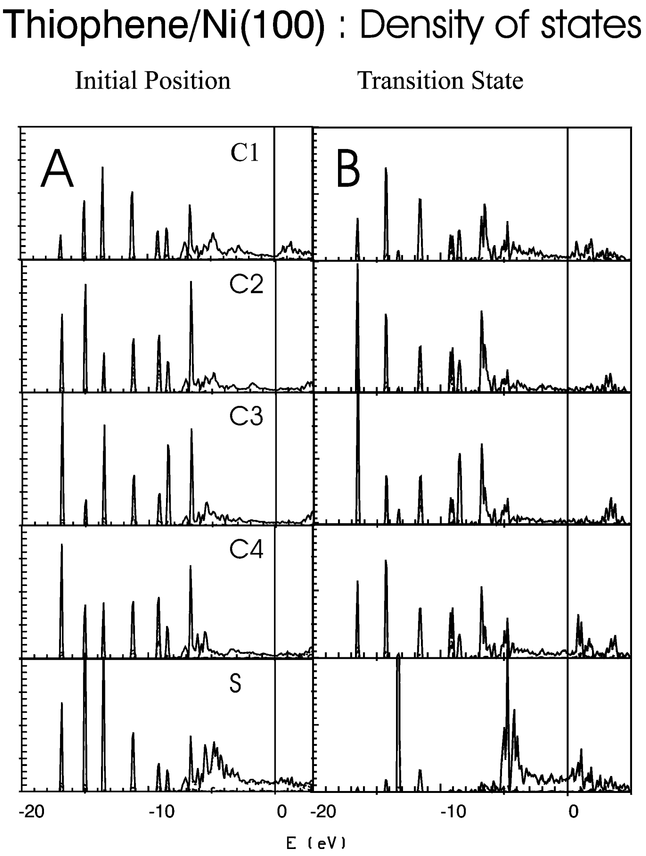

Fig. 4. Desulfurization of thiophene/Ni(100): local density of states for (A) the initial adsorption position and (B) the transition state A–TS projected onto the carbon (C) resp. sulfur (S) atom.

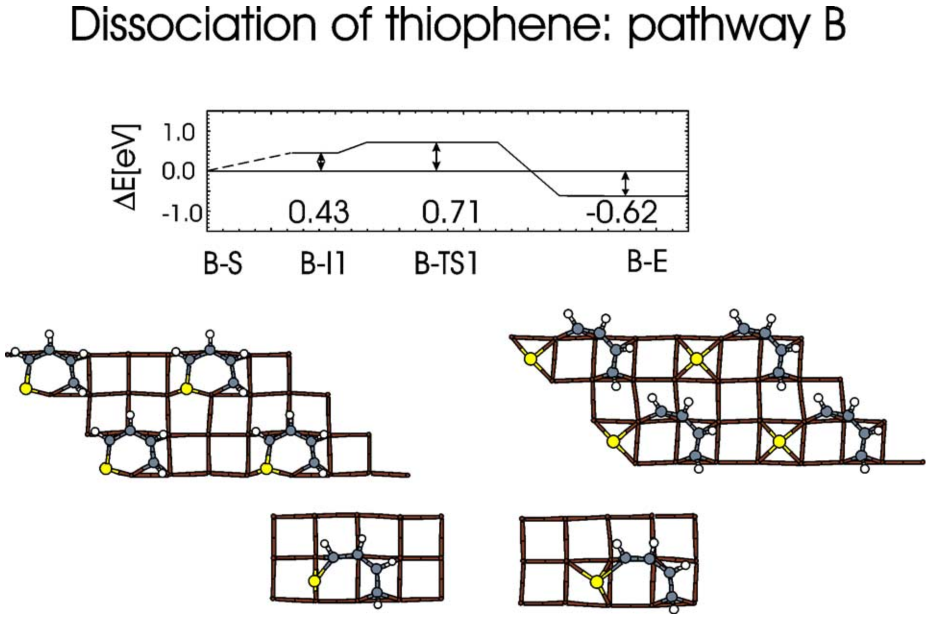

Fig. 5. Desulfurization of thiophene/Ni(100)–Path B: energetic profile along a complementary reaction path starting from the initial adsorption position of the reactant (A,B–S), followed by the metastable intermediate B–I1, the transition state (B–TS1), and the products in the final position (B–E).

After a further elongation of the sulfur–carbon bond to 2.11 Å the transition state (B–TS1) is reached (Fig. 6B). The bonds between the sulfur atom and the substrate show bond lengths of 2.15 Å, but the sulfur atom is already closer to the hollow site allowing an increased interaction with the substrate d-states. On a first glance the reaction pathway seems less favorable, yet the energetic profile of the process shows that the total barrier for the desulfurization $E_{\mathrm{barr}} = 0.71$ eV is lower and the energy gain compared to the initial adsorption position of $E_{\mathrm{reaction}} = 0.62$ eV is slightly higher than for the first reaction path. Although the sulfur atom has to be transferred between the bridge positions the main transition state of the reaction is found after crossing the second bridge site, the step of the cleavage of the remaining S–C bond.

A comparison of the transition states along the two competing reaction paths offers an explanation for the difference in the reaction barriers: the driving forces for the reaction are the energy gain by the reinforced interaction between the Ni substrate and the sulfur atom respectively the hydrocarbon chain, on the other hand the rearrangement of the molecule is mainly restricted by the energetic cost of the elongation of the C–S bond leading to its cleavage. In the initially discussed reaction path the weakening of the C–S bond results in a strengthening of C–Ni bond for the hydrocarbon fragment. Especially the carbon atom at the end of the chain, located close to a bridge site, is found to form an additional bond to the substrate which hinders the sulfur atom to gain energy by crossing the bridge site. In contrast to the initial reaction path the second pathway is based on a deformation of the thiophene molecule prior the cleavage of the S–C bond. As the bond lengths are kept nearly constant during the deformation of the molecule the energetic cost is rather low.

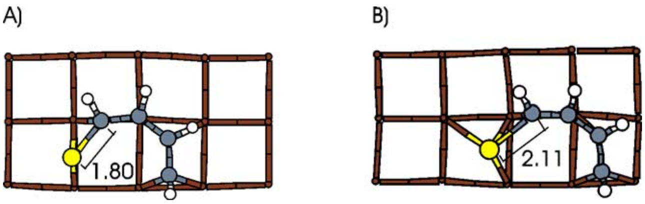

Fig. 6. Desulfurization of thiophene/Ni(100) along reaction path B: structure of (A) the intermediate and (B) the transition state of the reaction. Distances are given in Å.

5. Hydrodesulfurization of thiophene

As the cleavage of the S–C bond is obviously a crucial step in the desulfurization reaction, the S–C bond strength directly influences the reaction barrier. Hence the weakening of the bonds is correlated to an increasing reactivity.

The adsorption on the Ni(100) surface results in an occupation of the antibonding thiophene π^*-orbitals [18], thus causing a decline of the strength of the critical C–S bonds. A further step is the weakening of the S–C bond through a hydrogenation of the adsorbed thiophene molecule.

The following part is dedicated to the investigation of the influence of a hydrogenation of thiophene after the initial S–C bond scission, caused by the interaction with the surface, on the barrier for the dissociation.

5.1. Overview over the reaction pathway

In a recent ab initio DFT study Kresse [23] has shown that hydrogen dissociates on a clean Ni(100) surface over a substrate top position without a barrier, with a final adsorption

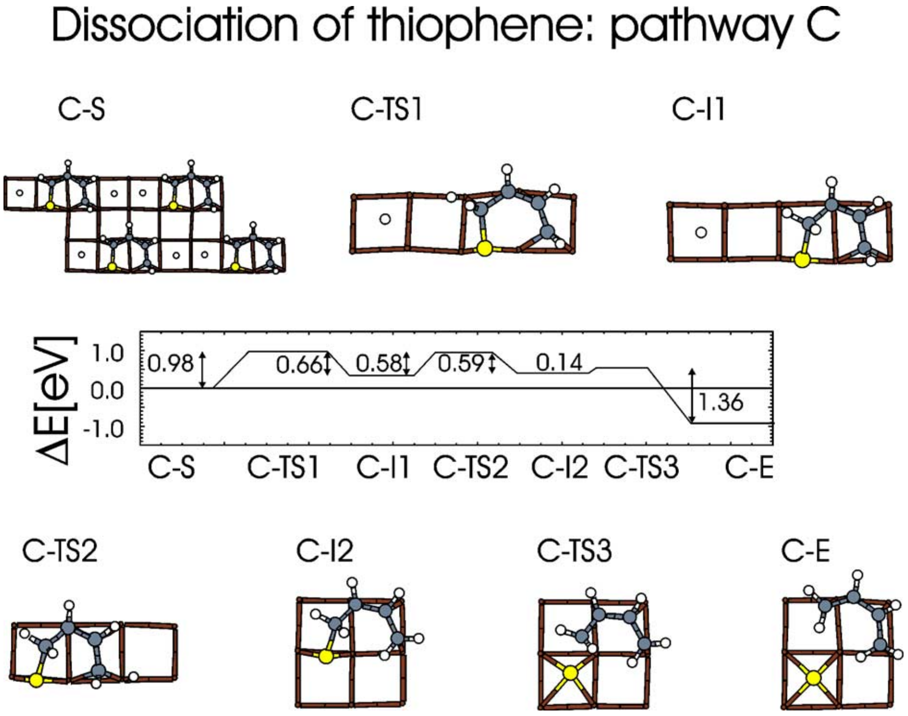

Fig. 7. Energetic profile of the reaction pathway for the hydrodesulfurization of thiophene/Ni(100): Starting from coadsorbed thiophene and hydrogen (C–S), the first transition state (C–TS1) for the initial hydrogenation of thiophene at the 2nd position, a reaction intermediate (C–I1), the following TS for the hydrogenation of the 5th position (C–TS2), SC_4H_6/Ni(100) (C–I2), the final S–C bond scission (C–TS3), and coadsorbed S and C_4H_6 (C–E).

site in the fourfold hollows. Hence the reaction path has been investigated starting from preadsorbed thiophene forming a $c(4 \times 4)$ superstructure and dissociatively coadsorbed H_2. Although the high coverage of the coadsorbed thiophene might create a barrier for the dissociation of the H_2 molecule like in the case of benzene + H2/Ni(111) [20], a possible barrier, presumably even lower than in the previous case due to the lower coverage and the more open surface, will be lower than the barriers for the desulfurization of the molecule. Although the availability of atomic hydrogen on the Ni(100) surface and the possible stabilization of the intermediates through the interaction with the metallic surface allow for a large number of reaction pathways and hydrogenation positions, one reaction pathway has been investigated in detail.

Fig. 7 gives an overview over the reaction scheme and the energetic profile along the reaction path: In the initial starting configuration (C–S), which has been taken as energetic reference, thiophene is preadsorbed forming a $c(4 \times 4)$ superstructure, and the additional hydrogen molecule has been dissociated into neighboring hollow sites. The first transition state (C–TS1) is encountered upon the initial hydrogenation step of the 2nd position of the thiophene molecule. With an energetic barrier of 0.98 eV this step is clearly rate-determining. After crossing the transition state the monohydrothiophene (C_4H_5S) is formed as a reaction intermediate (C–I1). Like in the case of the hydrogenation of benzene/Ni(111) the barrier for the second hydrogenation step (C–TS2), 0.58 eV, is significantly lower than the initial one. In the second reaction intermediate (C–I2) SC_4H_6 is adsorbed on the Ni surface. After the hydrogenation step, the barrier for the final S–C bond scission (C–TS3) is lowered to a value of 0.14 eV. The complete reaction results in an energy gain of 0.91 eV compared to the initial configuration.

Fig. 8 gives an overview of the structure of the molecule at the first transition state (C–TS1) of the hydrogenation: as the hydrogen atom has moved from the fourfold hollow position to the top position the surface-hydrogen bonds are weakened. The distance between the hydrogen atom and the nearest nickel atom is found to be $d(\text{H–Ni}) = 1.50$ Å, close to the calculated value for hydrogen adsorbed on a clean Ni(100) surface $d(\text{H–Ni})_{\text{top}} = 1.47$ Å [24]. The interaction between the hydrogen atom and the thiophene molecule is at this point rather weak: with a distance of $d(\text{H–C}) = 1.53$ Å between the hydrogen atom and the nearest carbon atom the C–H bond is only starting to form. The geometry at

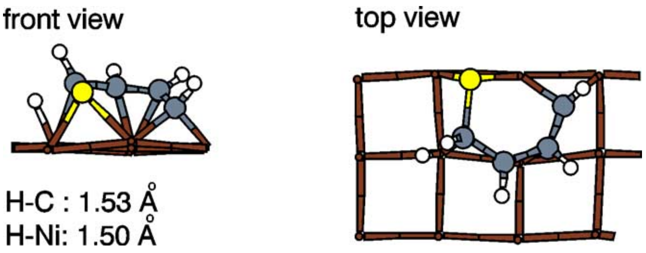

Fig. 8. Hydrogenation of thiophene/Ni(100): Structural characterization of the initial transition state (C–TS1). Distances are given in Å.

the second hydrogenation step is similar to the geometry of the initial step. In both cases the hydrogen atoms form chemisorptive bonds to the Ni substrate with a bond length of 1.50 Å, yet the second transition state is reached already at a larger C–H distance of 1.62 Å.

In the starting position of this reaction step the sulfur atom of the molecule is still located over the bridge site. In contrast to the initially adsorbed thiophene molecule the neighboring carbon atom is involved in a second C–H bond instead of a bond to the substrate. In addition the hydrogenation weakens the intramolecular carbon–sulfur and carbon–carbon bonds, which is reflected in bond lengths of $d(\text{C–S}) = 1.87$ Å, respectively $d(\text{C–C}) = 1.51$ Å. With bond lengths of 1.45 Å the two remaining carbon–carbon bonds are slightly stronger, still all intramolecular bond lengths are nearly unchanged compared to the intermediate of the first hydrogenation step. Both hydrogen pairs form an angle of $\angle(\text{HCH}) = 110°$.

The second hydrogenation step shows a drastic effect on the energetic barrier of the following desulfurization reaction (C–TS3). An analysis of the corresponding geometric structure (Fig. 9) illustrates that this is a rather late transition state: with a C–S bond length of 2.21 Å this bond is already broken, an observation confirmed by a strengthening of the neighboring C–C bond, which is contracted from 1.51 to 1.45 Å. As the carbon atom forming the C–S bond is not involved in a surface bond, the deformation of the reaction intermediate is facilitated. Hence the sulfur atom is already close to the hollow site at the transition state, resulting in a stronger interaction with the substrate, where the C–S bond is elongated to a value of $d(\text{C–S}) = 2.21$ Å compared to a value of $d(\text{C–S}) = 2.50$ Å for the corresponding reaction step for thiophene/Ni(100).

Therefore the hydrogenation of the molecule induces two effects: An electronic effect, as the intramolecular bonds are weakened, but also a steric effect as the flexibility of the molecule is enhanced with one of the bonds to the substrate replaced. The latter plays a central role as this reaction, as also shown by the previous reactions, is determined by the energy gain through the increased interaction of the hydrocarbon fragment and the sulfur atom with the substrate on the one hand and on the other hand the energetic cost of the deformation of the molecule

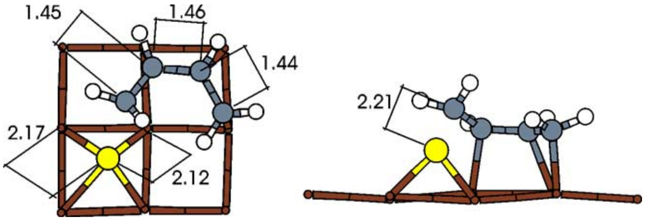

Fig. 9. Transition state (C–TS3) for the dissociation of 2,5-dihydrothiophene/Ni(100).

6. Conclusions

The initial adsorption geometry of thiophene/Ni(100) has been used as a starting point for the desulfurization of the thiophene molecule. After the desulfurization the sulfur atom is located in the hollow position with S–Ni bond lengths ranging from $d(\text{S–Ni}) = 2.16$ Å to $d(\text{S–Ni}) = 2.20$ Å, close to the calculated bond length of $d(\text{S–Ni}) = 2.18$ Å for a sulfur atom in a $p(2 \times 2)$ superstructure. The high thiophene coverage corresponding to the $c(4 \times 4)$ superstructure thus favors the desulfurization into two distinct hollow sites: one corresponding to a reaction mechanism based on a direct elongation of the sulfur–carbon bond, the other reaction path based on an initial deformation of the thiophene molecule transferring the sulfur atom between two bridge positions. The energetic barriers for the two processes are similar; still, with an energetic barrier of $\Delta E = 0.71$ eV, the second reaction mechanism is slightly favored over the first reaction mechanism ($\Delta E = 0.84$ eV) due to steric reasons.

The hydrogenolysis of the adsorbed thiophene molecule is found to lower the barrier for the S–C bond cleavage significantly to a value of $\Delta E = 0.14$ eV, as it not only weakens the remaining sulfur–carbon bond but decreases the energetic cost for the deformation of the thiophene molecule, thus allowing a transition state with the sulfur atom close to the hollow position. Yet an analysis of the investigated reaction path reveals that the initial step in the hydrogenation of the molecule has a barrier of $\Delta E = 0.98$ eV, higher than the barrier for the desulfurization of thiophene $\Delta E = 0.71$ eV.

Although the structure of the transition states for the initial hydrogenation step of benzene/Ni(111) and thiophene/Ni(100) are quite similar, the reaction barriers differ significantly. In both cases the hydrogenation of the molecule involves the breaking of a bond between the aromatic molecule and the surface. On the one hand the adsorption energies of the aromatics are higher for the more open Ni(100) surface than for the Ni(111) surface [19], on the other hand thiophene was found to form stronger bonds on the Ni(100) surface than on benzene [18].

Acknowledgment

This work has been supported by the Austrian Science Funds within the Science College “Computational Materials Science” (W004).

References

[1] B.J. Wiegand, C.M. Friend, Chem. Rev. 92 (1992) 491.
[2] H. Topsøe, B.S. Clausen, F.E. Massoth, in: Catalysis Science and Technology, Vol. 11, Springer, New York, 1996.
[3] D.D. Whitehurst, T. Isoda, I. Mochida, Adv. Catal. 42 (1998) 345.
[4] J. Kraus, M. Zdrazil, React. Catal. Lett. 6 (1977) 45.

[5] J.M.J.G. Lipsch, G.C.A. Schuit, J. Catal. 15 (1969) 179.
[6] J. Chen, L.M. Daniels, R.J. Angelici, J. Am. Chem. Soc. 113 (1991) 2544.
[7] D.R. Huntley, D.R. Mullins, M.P. Wingeier, J. Chem. Phys. 100 (1996) 19620.
[8] F. Zaera, E.B. Collin, J.L. Gland, Langmuir 3 (1987) 555.
[9] N.A. Khan, H.H. Hwu, J.G. Chen, J. Catal. 205 (2002) 259.
[10] M. Neurock, R.A. van Santen, J. Am. Chem. Soc. 116 (1994) 4427.
[11] G. Kresse, J. Hafner, Phys. Rev. B 47 (1993) C558.
[12] G. Kresse, J. Furthmüller, Comput. Mater. Sci. 6 (1996) 15.
[13] P.E. Blöchl, Phys. Rev. B 50 (1994) 17953.
[14] G. Kresse, D. Joubert, Phys. Rev. B 59 (1999) 1758.
[15] J.P. Perdew, J.A. Chevary, S.H. Voslo, K.A. Jackson, M.R. Pederson, D.J. Singh, C. Fiolhais, Phys. Rev. B 46 (1992) 6671.
[16] H.J. Monkhorst, J.D. Pack, Phys. Rev. B 13 (1976) 5188.
[17] M. Methfessel, A. Paxton, Phys. Rev. B 40 (1989) 3616.
[18] F. Mittendorfer, J. Hafner, Surf. Sci. 492 (2001) 27.
[19] F. Mittendorfer, J. Hafner, Surf. Sci. 472 (2001) 133.
[20] F. Mittendorfer, J. Hafner, J. Phys. Chem. 106 (2002) 13299.
[21] G. Mills, H. Jónsson, Phys. Rev. Lett. 72 (1994) 1124.
[22] J. Stöhr, E.B. Kollin, D.A. Fischer, J.B. Hastings, F. Zaera, F. Sette, Phys. Rev. Lett. 55 (1985) 1468.
[23] G. Kresse, Phys. Rev. B 62 (2000) 8295.
[24] G. Kresse, J. Hafner, Surf. Sci. 459 (2000) 287.